Polarization analysis of excitons in monolayer and bilayer transition-metal dichalcogenides

Hanan Dery[1,2,*] and Yang Song[1]
[1]*Department of Electrical and Computer Engineering, University of Rochester, Rochester, New York 14627, USA*
[2]*Department of Physics and Astronomy, University of Rochester, Rochester, New York 14627, USA*
(Received 23 June 2015; published 23 September 2015)

The polarization analysis of optical transitions in monolayer and bilayer transition-metal dichalcogenides provides invaluable information on the spin and valley (pseudospin) degrees of freedom. To explain optical properties of a given monolayer transition-metal dichalcogenide, one should consider (i) the order of its spin-split conduction bands, (ii) whether intervalley scattering is prone to phonon bottleneck, (iii) and whether valley mixing by electron-hole exchange can take place. Using these principles, we present a consistent physical picture that elucidates a variety of features in the optical spectra of these materials. We explain the differences between optical transitions in monolayer $MoSe_2$ and monolayer WSe_2, finding that indirect excitons in the latter correspond to several low-energy optical transitions that so far were attributed to excitons bound to impurities. A possible mechanism that can explain the vanishing polarization in $MoSe_2$ is discussed. Finally, we consider the effect of an out-of-plane electric field, showing that it can reduce the initial polarization of bright excitons due to a Rashba-type coupling with dark excitons.

DOI: 10.1103/PhysRevB.92.125431 PACS number(s): 78.55.−m, 71.35.−y, 71.70.Ej

I. INTRODUCTION

The valley and layer degrees of freedom in transition-metal dichalcogenide semiconductors have appealing pseudospin character, which can be used in applications and explorations of new physical phenomena [1–10]. The polarization of excitonic optical transitions provides invaluable information on these degrees of freedom [11–26]. Compared with typical semiconductors, electron-hole pairs are strongly bound in these materials due to relatively large effective masses of electrons and holes as well as moderate dielectric constants. Combined with the impeded Coulomb screening in two-dimensional systems, electron-hole pairs can remain bound at room temperature. Inspection of the excitonic luminescence in various transition-metal dichalcogenides reveals several particular features. Unlike other members of the family, the low-temperature luminescence from monolayer WSe_2 has several excitonic peaks closely below the energy of the free exciton (X_0) [17,22]. Following excitation by a linearly polarized light, only the free exciton retains such polarization. On the other hand, all excitons exhibit some polarization level when excited by a circularly polarized light. When performing the experiment with bilayers, the excitonic transitions retain the polarization of the excitation light [19–21]. Monolayer $MoSe_2$, on the other hand, shows a sharp spectrum merely consisting of free and charged exciton peaks. Both peaks show nearly no polarization regardless of the polarization of the excitation light (linear or circular) [23–25], and this behavior seems to persist in bilayer and trilayer $MoSe_2$ [27,28].

The purpose of our work is to try elucidating the above phenomena by providing a consistent physical picture. We explain the identity and polarization behavior of optical transitions in monolayer and bilayer transition-metal dichalcogenides (ML-TMDs and BL-TMDs), and shed light on the interplay between intervalley scattering and electron-hole exchange, and the role of an out-of-plane electric field. The findings are valuable for the interpretation of experimental results, and for elucidating the intrinsic limits for carrying pseudospin information in valleytronics [2,10].

Figure 1(a) shows low-energy valleys of electrons and holes in ML-TMDs. Due to the relatively large spin splitting in the valence band [30–38], we only consider the topmost spin-split band of holes in each valley. For electrons, on the other hand, the spin splitting is much smaller and we consider both spin bands in each valley. Using these electron and hole bands, we classify the so-called type-A excitons in ML-TMDs according to their spin and valley. Given that the orbital transition is dipole allowed, excitons are optically active (bright) or inactive (dark) when the spins of the electron in the conduction band and the missing electron in the valence band are parallel or antiparallel, respectively. In addition, excitons are said to be direct if the electron and hole reside in valleys that are centered around the same point in the Brillouin zone. Thus, direct excitons reside in the zone center (Γ valleys), while their electron and hole components can be from any part of the Brillouin zone (provided that $k_h - k_e \approx 0$). In ML-TMDs, a Γ-valley exciton comprises electron and hole from the K valley (or $-K$ valley). Similarly, excitons are said to be indirect if the electron and hole are from opposite valleys (e.g., electron from K and hole from $-K$). Accordingly, radiative recombination of an indirect bright exciton involves the assistance of a phonon or point defect in order to obey or alleviate crystal-momentum conservation, respectively [39–42].

Using the above classifications, Fig. 1(b) shows the resulting low-energy bands of type-A excitons in ML-TMDs. The order of bright and dark exciton bands follows the order of the spin-split conduction bands used in Fig. 1(a). The direct bright exciton has lower energy than the direct dark exciton and vice versa for the indirect excitons. This ordering applies for ML-$MoSe_2$, while its reverse applies for ML-WSe_2. As will be explained, this difference can have a profound effect on the luminescence. Below, we briefly discuss the excitation of type-A excitons and their relaxation to the bottom of the bands. We then focus on the identity and polarization of the ensuing optical transitions.

*hanan.dery@rochester.edu

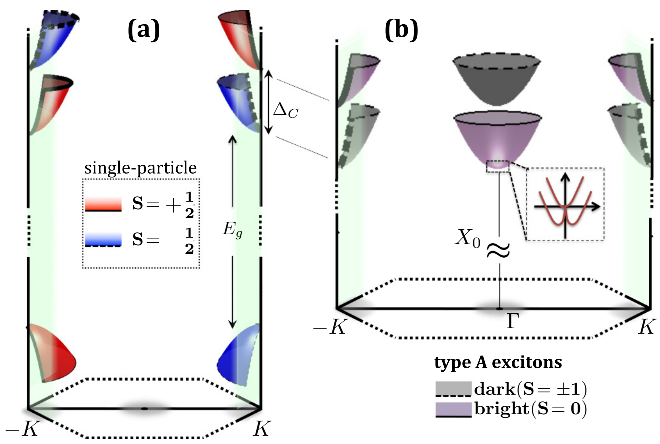

FIG. 1. (Color online) (a) Low-energy band diagrams of electrons and holes in ML-TMDs. The spin order of conduction bands is that of molybdenum-based TMDs, while the opposite order applies for tungsten-based TMDs [32–34]. The spin splitting in the conduction band, Δ_c, is much smaller than the energy gap (see Table I). (b) The resulting bands of type-A excitons. The dark-bright exciton splitting is governed by Δ_c. Zone-center bands (direct excitons) are doubly degenerate and denote pairs from K or $-K$ valleys. The electron-hole exchange lifts the degeneracy in the bottom of the direct bright band as shown in the highlighted box [29]. Indirect exciton bands in the edge valleys are singly degenerate where each denotes a specific combination of valley and spin for the electron and hole.

Light absorption generates primarily direct bright excitons due to their largest optical transition amplitude. The energy degeneracy of the K and $-K$ valleys results in doubly degenerate bands of direct excitons, which for the bright branch are distinguished by the valley index or equivalently by light helicity ($m_l = \pm 1$). Accordingly, linearly polarized light excites a valley superposition of the $m_l = \pm 1$ states, while circularly polarized light excites one of them. In either case, photoluminescence (PL) experiments show that the X_0 peak, which is related to energy-relaxed direct bright excitons, largely retains the polarization of the excitation light in all but SL-$MoSe_2$ [17–20,22–28]. The conservation of linear polarization indicates faster intravalley relaxation of hot excitons compared with the intervalley scattering of their electron components. The conservation of circular polarization indicates that the intravalley relaxation is also faster than the electron-hole exchange effect. The latter mixes the $m_l = \pm 1$ states [43]. While the energy relaxation of hot excitons is not the focus of this study, we mention a few important relaxation channels in Appendix A with emphasis on the interaction of excitons with long-wavelength optical phonons.

II. EFFECT OF ELECTRON-HOLE EXCHANGE

Following polarized excitation, the luminescence from TMDs can become unpolarized if the time scale for exchange-induced valley mixing is faster than the recombination lifetime. We follow the theory of Yu *et al.* [29] and explain the effect of electron-hole exchange on direct bright excitons in TMDs. Away from the Γ point, the exchange lifts the energy degeneracy according to $E_0 + E_k \pm J_0 k$ where the three terms correspond to edge, kinetic, and exchange energies of direct bright excitons [see highlighted box in Fig. 1(b)]. The exchange-induced splitting depends linearly on crystal momentum (k), where $J_0 \sim 1$ eV Å [29]. In the light cone, where $k \sim 2\pi/\lambda_{\text{light}}$, the splitting is of the order of $\sim$1 meV. The resulting oscillations between components of a prepared state can therefore have a period of few ps (Dyakonov-Perel-type precession of the valley degree of freedom) [43–45]. This time scale is significantly faster than in typical semiconductors due to the tight overlap between the wave functions of the electron and hole (e.g., an unscreened exciton extends over areas of $\sim$1 nm^2 in MoS_2 vs 100 nm^2 in GaAs). The net effect is that polarization of the X_0 peak drops if the valley mixing, induced by the electron-hole exchange, is faster than recombination. Applying a large magnetic field can increase the circular polarization due to the suppression of the exchange-induced valley mixing by lifting the Γ-point energy degeneracy of direct bright excitons [23,25].

III. PHOTOLUMINESCENCE IN ML-WSe_2

In this material, the indirect bright branch has lower energy than the direct bright branch. Figure 2 shows the energy diagram along with processes that govern the luminescence. Following Table I, ML-WSe_2 is the only member in which the dark-bright energy splitting is larger than the energy of the K-point phonon needed for intervalley scattering (i.e., in which $|\Delta_c| > E_{K_3}$). Accordingly, energy-relaxed direct bright excitons do not experience a phonon bottleneck in ML-WSe_2 and eventually become indirect. This physical picture means that optical transitions across the direct gap (X_0) represent radiative recombination events just before direct bright excitons turn indirect. Accordingly, X_0 can retain linear polarization since its luminescence takes place before the intervalley scattering (i.e., the valley superposition is preserved). Similarly, X_0 can retain circular polarization if the time scale for intervalley scattering is faster than that for

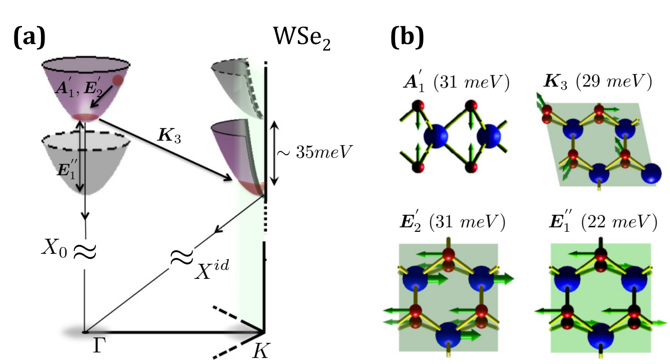

FIG. 2. (Color online) (a) Luminescence process in monolayer WSe_2. After energy relaxation to the bottom of the direct bright branch, excitons either recombine or scattered to other branches. Optical phonon modes that participate in the intravalley and intervalley relaxation are indicated, and the corresponding atomic displacements and phonon energies are shown in (b). Direct optical transitions (X_0) can retain the excitation polarization, while indirect ones (X^{id}) can do so only for circularly polarized excitation (see text).

TABLE I. Conduction-band spin splitting and pertinent phonon energies in ML-TMDs. Figure 2(b) shows the atomic displacements that correspond to these phonon modes. In Koster notation, $A_1' \to \Gamma_1$, $E_1'' \to \Gamma_5$, and $E_2' \to \Gamma_6$. The spin splitting of the conduction band, whose existence is mandated by group theory [47], was not directly measured to date. Its shown values are from density functional theory calculations.

	WSe_2	$MoSe_2$	WS_2	MoS_2	Ref.
Δ_c (meV)	− 37	21	− 32	3	[30–34]
$E_{A_1'}$ (meV)	31	30	52	51	[35–37]
$E_{E_2'}$ (meV)	31	36	45	49	[35–37]
$E_{E_1''}$ (meV)	22	21	37	36	[35–37]
E_{K_3} (meV)	29	35	43	42	[35–38]

electron-hole exchange. This behavior is indeed corroborated in experiments [17,22,46].

IV. PHOTOLUMINESCENCE OF INDIRECT EXCITONS IN ML-WSe_2

Figure 2(a) shows that in addition to X_0, the PL in ML-WSe_2 includes optical transitions from indirect bright excitons (X^{id}). At elevated temperatures, the populations of direct and indirect bright excitons become comparable (absorption and emission of intervalley phonons have equivalent amplitudes). As a result, the PL is dominated by the direct exciton transition (X_0) due to its stronger optical transition amplitude. At low temperatures, on the other hand, one can expect measurable PL from indirect bright excitons due to their evidently larger population (intervalley phonon absorption becomes negligible). In addition to population densities and optical-transition amplitudes, the lifetime of direct and indirect bright excitons is affected by nonradiative recombination centers. Whereas the fairly low yield of the PL in ML-TMDs suggests that these centers affect the recombination of both exciton types, the signature on the lifetime of indirect excitons is expected to be stronger due their intrinsically longer radiative time scales.

Recalling that optical transitions of indirect bright excitons require assistance of phonons or point defects, we can expect several of these peaks. The energy of the highest indirect peak is $X_i^{id} = X_0 - \Delta_c$, and it is associated with an impurity-assisted optical transition mediated by elastic scattering of point defects. The energy of the second highest peak is $X_K^{id} = X_0 - \Delta_c - E_{K_3}$, and it is associated with a phonon-assisted optical transition via zone edge modes with K_3 symmetry [47]. The conservation of crystal momentum due to translation symmetry is enabled by virtual intervalley scattering to the light-cone region in the bottom of the direct bright exciton band. Finally, one can expect weaker peaks at larger phonon replicas such as $X_{K+\Gamma}^{id} = X_0 - \Delta_c - E_{K_3} - E_{A_1'/E_2'}$ which involves emission of zone-edge and zone-center phonon modes [see Fig. 2(b) for these phonon types]. Here the zone-edge phonon virtually scatters the exciton to the zone center, where it can interact with another long-wavelength optical phonon (Raman active modes). Inspection of the parameters of ML-WSe_2 in Table I reveals that X_i^{id}, X_K^{id}, and $X_{K+\Gamma}^{id}$ should appear between ∼35 meV and ∼100 meV below X_0.

V. POLARIZATION OF INDIRECT EXCITONS IN ML-WSe_2

Indirect excitons do not preserve linear polarization but can keep circular polarization. By definition, the transition of excitons from the direct branch in which they were generated to the indirect branch involves intervalley scattering. As a result, the prepared valley superposition in the case of an excitation with a linearly polarized light is destroyed. On the other hand, retaining circular polarization is possible due to combination of two factors. First, the holes keep their spin throughout all relaxation processes (until the radiative recombination). Second, the indirect exciton bands are not prone to electron-hole exchange since they are singly degenerate [47]. Previous experiments attributed the optical transitions below X_0 in ML-WSe_2 to excitons bound to impurities [17,22]. The energy difference from X_0 was then associated with the binding energy of the exciton to the impurity. We argue that some of these peaks should be attributed to the indirect bright excitons X_i^{id}, X_K^{id}, and $X_{K+\Gamma}^{id}$. Not only do their polarizations and energies fit the experiment, our physical picture can explain why these peaks are observed in ML-WSe_2 but not in ML-$MoSe_2$. If binding to impurities is the origin, then one is confronted with the fact that similar peaks are not seen in ML-$MoSe_2$.

The PL due to indirect excitons is weakened when they can be thermally excited to the direct exciton branch in which the optical transitions are much stronger. This weakening thus follows the Bose-Einstein distribution of intervalley phonons, which seems to be in agreement with empirical results [22,48,49]. Previously, theoretical support to this temperature dependence was found in the small dissociation energy of acceptor-bound or donor-bound excitons compared with the dissociation energy of other charged exciton complexes [50].

VI. PHOTOLUMINESCENCE IN BL-TMDS

The physical picture presented so far implies that optical transitions associated with X_0 are expected to preserve the excitation polarization in BL-TMDs (linear or circular). Contrary to ML-TMDs, bilayers are *indirect* band-gap semiconductors in which the interlayer coupling is mostly governed by p orbitals of the chalcogen atoms. Therefore, the coupling only slightly shifts the energy gap of the K point whose electron and hole states are mainly governed by the d orbitals of transition-metal atoms. The result is that ground-state excitons are indirect, and their energy is below that of either direct or *indirect* excitons that comprise electrons and holes of the K and $-K$ valleys. The radiative recombination of direct excitons that govern X_0 in bilayers is therefore limited to the time window between their excitation to the direct bright branch and intervalley scattering to the *indirect* branch. A short time window can readily suppress the exchange-induced valley mixing of direct bright excitons. This physical picture explains the results of several recent experiments with bilayers, in which X_0 retained the excitation polarization [19–21].

VII. ANOMALOUS BEHAVIOR OF $MoSe_2$

Contrary to the cases of WS_2, WSe_2, and MoS_2, the PL spectrum of type-A excitons in $MoSe_2$ is unpolarized even when the polarized excitation is close to the X_0 transition. This anomalous behavior seems to persist in monolayers [23–26], bilayers [27,28], and multilayers [28]. As shown in Fig. 1, the direct bright branch is lower in energy than the direct dark branch in this compound. Therefore, indirect bright excitons should not affect the PL spectrum due to their small population and weak optical-transition amplitude. It is tempting to justify the vanishing polarization of direct bright excitons by arguing that the valley mixing, induced by electron-hole exchange, is faster than recombination or intervalley scattering. However, time-resolved PL experiments reveal recombination times of the order of a few ps [24], similar to those found in other TMDs [18,22]. In addition, a recent PL experiment in ML-$MoSe_2$ showed that when the optical excitation is from the bottom spin-split valence band to the conduction band (type-B excitons), the luminescence of these higher-energy excitons remains polarized [26]. This observation suggests that the electron-hole exchange of type-B excitons is not efficient within the time window between their excitation and energy relaxation to the type-A branch. Importantly, the magnitude of electron-hole exchange of type-A excitons should be similar to that of type-B excitons on account of their similar symmetries and atomic orbitals. All these facts imply that the enhanced effect of the electron-hole exchange in $MoSe_2$ compared with other TMDs is not likely to be the cause for the PL's vanishing polarization.

We conjecture that the anomalous behavior in $MoSe_2$ can be reasoned by polaron-induced coherent coupling between the direct branches of bright and dark excitons. By inspecting the transformation properties of these excitons, they can only be coupled by the E_1'' phonon mode whose corresponding atomic displacement is shown in Fig. 2(b) [47]. Of all TMDs, the energy of this phonon resonates with the conduction-band spin splitting only in $MoSe_2$ ($\Delta_c \simeq E_{E_1''}$; see Table I). A possible outcome is a polaron-induced coupling that drives coherent oscillations between the direct-bright and direct-dark excitons, where on each return to the bright branch the helicity changes sign (Rabi oscillations in a two-level system where each level is doubly degenerate). This process can be accountable for the vanishing polarization if the electron-phonon coupling amplitude is strong enough to support sub-1-ps oscillations. The physics should be similar in ML-$MoSe_2$ and multilayer-$MoSe_2$ since the Γ-point phonon energies and K-point splitting of the conduction band hardly change with the number of layers.

VIII. “BRIGHTENING” DARK EXCITONS IN ML-TMDS

Spin flips of the electron or hole component induce transitions between bright and dark excitons [47]. The other way to couple dark and bright excitons in monolayers, where space inversion is not respected, is via the presence of an out-of-plane electric field (e.g., by a gate voltage or charged impurities in the substrate).

To correctly quantify the resulting Rashba-type coupling between bright and dark components of direct excitons, we follow their transformation properties according to the group theory analysis in Ref. [47]. The resulting Hamiltonian matrix of direct excitons reads

$$H = \begin{pmatrix} H_b & H_R \\ H_R^* & H_d \end{pmatrix}. \tag{1}$$

The upper diagonal block belongs to bright excitons [23,29],

$$H_b = \frac{\hbar^2 k^2}{2M}\mathcal{I} + J_0 k(\cos 2\theta\sigma_x + \sin 2\theta\sigma_y) + \eta_b B_z\sigma_z, \tag{2}$$

where we have incorporated the possibility of an out-of-plane magnetic field in addition to exchange and kinetic terms. M is the free exciton mass (about twice the electron mass in TMDs), $\mathbf{k} = k(\cos\theta, \sin\theta)$, and $\eta_b \approx 2\mu_B$ due to valence-band orbitals of the transition-metal atoms. Working in this subspace (in which basis states transform as Γ_6), one can quantify the competition between electron-hole exchange and the magnetic field. The lower diagonal block in Eq. (1) is of dark excitons,

$$H_d = \Delta_{bd} + \frac{\hbar^2 k^2}{2M}\mathcal{I} + (J_d + \eta_d B_z)\sigma_z, \tag{3}$$

where $\Delta_{bd} \approx \Delta_c$ is the bright-dark energy splitting (we consider the energies of the $k = 0$ states in the bright branch as the reference level). The last term includes the short-range exchange interaction as well as Zeeman terms. The existence of exchange-induced splitting is supported by the fact that the basis states in the dark branch transform as one-dimensional rather than two-dimensional irreducible representations (Γ_3 and Γ_4 rather than Γ_5). The Zeeman term of dark excitons, $\eta_d \approx 4\mu_B$, has contributions from the spin and valence-band orbitals of the transition-metal atoms. Finally, the off-diagonal block in Eq. (1) represents the Rashba coupling between bright and dark excitons,

$$H_R = \alpha_R k E_z \begin{pmatrix} \exp(-i\theta) & \exp(-i\theta) \\ -\exp(i\theta) & \exp(i\theta) \end{pmatrix}, \tag{4}$$

where E_z is the out-of-plane electric field and α_R is the Rashba coefficient (see Appendix B for its analytical expression) [51].

To see the coupling between bright and dark excitons, it is sufficient to diagonalize Eq. (1) by neglecting the magnetic and exchange terms (their energy scales are smaller than the bright-dark energy splitting). The new dark states are “brightened” by the E field according to

$$\widetilde{\Psi}_{d1,d2} \approx \Psi_{d1,d2} + \frac{\alpha_R k E_z}{\Delta_{bd}}\left(\Psi_R e^{-i\theta} \pm \Psi_L e^{i\theta}\right), \tag{5}$$

where $\Psi_{R,L}$ are the basis states of bright excitons (right or left helicity), and $\Psi_{d1,d2}$ are the basis states of dark excitons without the E field. Similar expressions can be derived for bright excitons. The E-field induced brightening of dark excitons (and darkening of bright excitons) becomes evident away from the zone center. This mixing degrades the attainable valley polarization upon excitation above resonance in ML-TMDs.

IX. CONCLUDING REMARKS

We have attempted to elucidate many of the features of optical transitions in transition-metal dichalcogenides. An important effect is that energy-relaxed direct bright excitons, which correspond to the so-called X_0 peak, can retain the linear or circular polarization of the excitation light when two intrinsic conditions apply. The first one is that their energy is above that of indirect bright excitons, and the second one is that intervalley transitions are not impeded by a phonon bottleneck.

These conditions apply in monolayer WSe_2 for which we have associated several of the observed optical transitions with indirect bright excitons, and explained their polarization behavior. These conditions can also be applied in multilayers if the recombination lifetime of direct bright excitons is limited by an ultrafast time window between excitation and intervalley scattering to the low-energy indirect gap.

The anomalous vanishing polarization in monolayer and multilayer $MoSe_2$ remains an open question. We have alluded to a subtlety in the band diagram of excitons in $MoSe_2$ by noticing that the energy splitting between dark and bright exciton branches resonates with the energy of the phonon that couples these branches. This resonance condition, not met in other transition-metal dichalcogenides, can result in vanished polarization due to polaron-induced Rabi oscillations between dark and bright excitons.

Finally, we have presented the Rashba coupling between dark and bright components of direct excitons in the presence of an out-of-plane electric field. The coupling is amplified away from the zone center, and therefore can affect the initial polarization degree of excited electron-hole pairs.

ACKNOWLEDGMENTS

We are grateful for many useful discussions with X. Xu who proposed this topic. We are thankful to A. Hanbicki, A. M. Jones, J. Shan, K. F. Mak, and N. Vamivakas for sharing valuable experimental results prior to their publication. Finally, we are grateful to W. Yao for illuminating discussions on the effect of electron-hole exchange. This work was supported by the Department of Energy under Contract No. DE-SC0014349, National Science Foundation under Contract No. DMR-1503601, and the Defense Threat Reduction Agency under Contract No. HDTRA1-13-1-0013.

APPENDIX A: ENERGY RELAXATION OF HOT EXCITONS

The energy relaxation is mediated by interaction of excitons with other excitons, free charges, impurities, or phonons. Relaxation via exciton-exciton or exciton-plasmon scattering becomes relevant for high-intensity excitation [52,53], or when the background-charge density is large [54]. Relaxation can also be governed by the displacement of point-defect impurities [55], similar to the case of interface states in quantum dots [56,57]. Here we will focus, however, on the intrinsic relaxation in high-quality crystals subjected to weak excitation and low background density of free charges. In this case, emission of long-wavelength optical phonons is the most relevant relaxation path, and it can take place in less than 1 ps if only a handful of phonon emissions are needed in order to reach the bottom of the type-A exciton branch.

From symmetry, only the Raman-active modes $A_1^{'}$ and $E_2^{'}$, shown in Fig. 2(b), are involved in intravalley energy relaxation (Γ_1 and Γ_6 in Koster notation). The $A_1^{'}$ mode corresponds to thickness fluctuations while the $E_2^{'}$ mode corresponds to in-phase motion of the chalcogen atoms in the plane of the layer. The phonon-exciton interaction in both cases have long-range and short-range components. The long-range interactions are due to Frohlich-type coupling between the excitons and the in-plane macroscopic electric field generated by both atomic displacements in the long-wavelength limit. The exciton does not change its polarization state since both long-range interactions transform as the identity irreducible representation. The interaction of neutral excitons with the long-range macroscopic field is expected to be weak due to similar but opposite-sign contributions from the electron and hole components.

The short-range interactions of excitons with the $A_1^{'}$ and $E_2^{'}$ phonon modes have opposite polarization effects. The exciton does not change its polarization state by the short-range interaction with $A_1^{'}$ modes, since the corresponding atomic displacement transforms as the identity irreducible representation. The amplitude of this short-range interaction is governed by the deformation potential of the thickness fluctuations [58,59]. On the other hand, the exciton changes its polarization state due to the short-range interaction with $E_2^{'}$ modes since their atomic displacement complies with the transformation properties of off-diagonal Pauli matrices (σ_x and σ_y) [47]. This scattering therefore flips the helicity (valley state) of bright excitons in the case of a circularly polarized prepared state, and destroys the polarization in the case of a linearly polarized prepared state. This behavior was indeed corroborated in a recent experiment [60].

APPENDIX B: RASHBA COEFFICIENT

Using $\mathbf{k}\cdot\mathbf{p}$ state expansion, the Rashba coefficient can be written as

$$\alpha_R \approx \frac{ie\hbar}{m}\left[\frac{\langle\Psi_{6,x}|z|\Psi_5\rangle\langle\Psi_5|p_y|\Psi_3\rangle}{\varepsilon_6-\varepsilon_5} + \frac{\langle\Psi_{6,x}|p_y|\Psi_2\rangle\langle\Psi_2|z|\Psi_3\rangle}{\varepsilon_6-\varepsilon_2}\right], \tag{B1}$$

where Ψ_i represent the basis states of irreducible representations Γ_i in Koster notation. Γ_6 corresponds to bright excitons where $2\Psi_{6,x} = \Psi_{6,L} + \Psi_{6,R}$. The dark excitons are represented by Γ_3. Equivalent expressions can be derived with the help of Ψ_4 and $\Psi_{6,y}$ (the other pair of dark and bright states). The symmetry allowed intermediate states are represented by $\Gamma_{2,5}$ irreducible representations. Type-B dark excitons, which belong to Γ_5, seem to contribute the most since the energy denominator in Eq. (B1) becomes the valence-band spin splitting, which is evidently smaller than for all other remote bands with $\Gamma_{2,5}$ symmetries. The expression for α_R suggests that it scales linearly with the spin mixing of the conduction-band components of exciton states. The reason is that initial ($\Psi_{3,4}$) and final (Ψ_6) states have opposite spins for conduction components. In deriving the expression for α_R, we have used $\langle\Psi_{6,x} \pm i\Psi_{6,y}|\ldots|\Psi_4\rangle \sim \Gamma_5 \sim (x \mp iy)z$ and $\langle\Psi_{6,x} \pm i\Psi_{6,y}|\ldots|\Psi_3\rangle \sim \Gamma_5 \sim (\pm x - iy)z$. Finally, we note that α_R can be extracted from *ab initio* techniques by fitting a $(\alpha_R E_z k)^2/\Delta_c$ component in the conduction-band energy dispersion as a function of E_z. Kormanyos *et al.* found that the Rashba effect is weaker than the one observed in InAs or InSb quantum wells [51]. This property stems from the fact that the conduction-band minimum is spin split in TMDs but not in III-V semiconductors. In other words, whereas gate voltages that result in $E_z \sim 1$ V/nm can render a significant Rashba effect in the vicinity of a spin-degenerate point (e.g., zone center in III-V semiconductors), such a field would still constitute a relatively weak perturbation in TMDs since their conduction-band minimum at the K point is spin split by the spin-orbit coupling.

---

[1] K. F. Mak, C. Lee, J. Hone, J. Shan, and T. F. Heinz, Phys. Rev. Lett. **105**, 136805 (2010).
[2] D. Xiao, G.-B. Liu, W. Feng, X. Xu, and W. Yao, Phys. Rev. Lett. **108**, 196802 (2012).
[3] S. Cahangirov, C. Ataca, M. Topsakal, H. Sahin, and S. Ciraci, Phys. Rev. Lett. **108**, 126103 (2012).
[4] Q. H. Wang, K. Kalantar-Zadeh, A. Kis, J. N. Coleman, and M. S. Strano, Nat. Nanotechnol. **7**, 699 (2012).
[5] H.-Z. Lu, W. Yao, D. Xiao, and S.-Q. Shen, Phys. Rev. Lett. **110**, 016806 (2013).
[6] Z. Gong, G.-B. Liu, H. Yu, D. Xiao, X. Cui, X. Xu, and W. Yao, Nat. Commun. **4**, 2053 (2013).
[7] S. Tongay, J. Zhou, C. Ataca, J. Liu, J. S. Kang, T. S. Matthews, L. You, J. Li, J. C. Grossman, and J. Wu, Nano Lett. **13**, 2831 (2013).
[8] K. Goodfellow, R. Beams, C. Chakraborty, L. Novotny, and A. N. Vamivakas, Optica **1**, 149 (2014).
[9] X. Xu, W. Yao, D. Xiao, and T. F. Heinz, Nat. Phys. **10**, 343 (2014).
[10] K. F. Mak, K. L. McGill, J. Park, and P. L. McEuen, Science **344**, 1489 (2014).
[11] H. Zeng, J. Dai, W. Yao, D. Xiao, and X. Cui, Nat. Nanotechnol. **7**, 490 (2012).
[12] K. F. Mak, K. L. He, J. Shan, and T. F. Heinz, Nat. Nanotechnol. **7**, 494 (2012).
[13] T. Cao, G. Wang, W. Han, H. Ye, C. Zhu, J. Shi, Q. Niu, P. Tan, E. Wang, B. Liu, and J. Feng, Nat. Commun. **3**, 887 (2012).
[14] G. Sallen, L. Bouet, X. Marie, G. Wang, C. R. Zhu, W. P. Han, Y. Lu, P. H. Tan, T. Amand, B. L. Liu, and B. Urbaszek, Phys. Rev. B **86**, 081301(R) (2012).
[15] G. Kioseoglou, A. T. Hanbicki, M. Currie, A. L. Friedman, D. Gunlycke, and B. T. Jonker, Appl. Phys. Lett. **101**, 221907 (2012).
[16] K. F. Mak, K. He, C. Lee, G. H. Lee, J. Hone, T. F. Heinz, and J. Shan, Nature Materials **12**, 207 (2013).
[17] A. M. Jones, H. Yu, N. J. Ghimire, S. Wu, G. Aivazian, J. S. Ross, B. Zhao, J. Yan, D. G. Mandrus, D. Xiao, W. Yao, and X. Xu, Nat. Nanotechnol. **8**, 634 (2013).
[18] D. Lagarde, L. Bouet, X. Marie, C. R. Zhu, B. L. Liu, T. Amand, P. H. Tan, and B. Urbaszek, Phys. Rev. Lett. **112**, 047401 (2014).
[19] B. Zhu, H. Zeng, J. Dai, Z. Gong, and X. Chi, Proc. Natl. Acad. Sci. USA **111**, 11606 (2014).
[20] A. M. Jones, H. Yu, J. S. Ross, P. Klement, N. J. Ghimire, J. Yan, D. G. Mandrus, W. Yao, and X. Xu, Nat. Phys. **10**, 130 (2014).
[21] G. Wang, X. Marie, L. Bouet, M. Vidal, A. Balocchi, T. Amand, D. Lagarde, and B. Urbaszek, Appl. Phys. Lett. **105**, 182105 (2014).
[22] G. Wang, L. Bouet, D. Lagarde, M. Vidal, A. Balocchi, T. Amand, X. Marie, and B. Urbaszek, Phys. Rev. B **90**, 075413 (2014).
[23] D. MacNeill, C. Heikes, K.-F. Mak, Z. Anderson, A. Kormányos, V. Zólyomi, J. Park, and D. C. Ralph, Phys. Rev. Lett. **114**, 037401 (2015).
[24] G. Wang, E. Palleau, T. Amand, S. Tongay, X. Marie, and B. Urbaszek, Appl. Phys. Lett. **106**, 112101 (2015).
[25] G. Wang, L. Bouet, M. M. Glazov, T. Amand, E. L. Ivchenko, E. Palleau, X. Marie, and B. Urbaszek, 2D Mater. **2**, 034002 (2015).
[26] A. Zhang, J. Fan, Y. Li, J. Ji, G. Zhao, T. Xia, T. Yan, X. Zhang, W. Zhang, X. Wang, and Q. Zhang, arXiv:1503.08631.
[27] Xiaodong Xu (private communication); PL experiments show unpolarized spectrum of both the neutral and charged excitons in ML-$MoSe_2$ and BL-$MoSe_2$.
[28] Nick Vamivakas (private communication); PL experiments show unpolarized spectrum of both the neutral and charged excitons in ML-$MoSe_2$, BL-$MoSe_2$, as well as trilayer $MoSe_2$.
[29] H. Yu, G.-B. Liu, P. Gong, X. Xu, and W. Yao, Nat. Commun. **5**, 3876 (2014).
[30] T. Cheiwchanchamnangij, W. R. L. Lambrecht, Y. Song, and H. Dery, Phys. Rev. B **88**, 155404 (2013).
[31] K. Kośmider and J. Fernández-Rossier, Phys. Rev. B **87**, 075451 (2013).
[32] G.-B. Liu, W.-Y. Shan, Y. Yao, W. Yao, and D. Xiao, Phys. Rev. B **88**, 085433 (2013).
[33] K. Kośmider, J. W. González, and J. Fernández-Rossier, Phys. Rev. B **88**, 245436 (2013).
[34] A. Kormányos, G. Burkard, M. Gmitra, J. Fabian, V. Zólyomi, N. D. Drummond, and V. Fal'ko, 2D Mater. **2**, 022001 (2015).
[35] A. Molina-Sánchez and L. Wirtz, Phys. Rev. B **84**, 155413 (2011).
[36] H. Terrones, E. Del Corro, S. Feng, J. M. Poumirol, D. Rhodes, D. Smirnov, N. R. Pradhan, Z. Lin, M. A. Nguyen, A. L. Elias, T. E. Mallouk, L. Balicas, M. A. Pimenta, and M. Terrones, Sci. Rep. **4**, 4215 (2014).
[37] A. Berkdemir, H. R. Gutiérrez, A. R. Botello-Méndez, N. Perea-López, A. L. Elias, C.-I. Chi, B. Wang, V. H. Crespi, F. López-Urías, J.-C. Charlier, H. Terrones, and M. Terrones, Sci. Rep. **3**, 1755 (2013).
[38] C. Ataca, H. Şahin, and S. Ciraci, J. Phys. Chem. C **116**, 8983 (2012).
[39] M. Lax and J. J. Hopfield, Phys. Rev. **124**, 115 (1961).
[40] P. Y. Yu and M. Cardona, *Fundamentals of Semiconductors*, 3rd ed. (Springer, Berlin, 2005), Chap. 6.
[41] P. Li and H. Dery, Phys. Rev. Lett. **105**, 037204 (2010).
[42] P. Li, D. Trivedi, and H. Dery, Phys. Rev. B **87**, 115203 (2013).
[43] M. Z. Maialle, E. A. de Andrada e Silva, and L. J. Sham, Phys. Rev. B **47**, 15776 (1993).
[44] M. I. Dyakonov and V. I. Perel, Sov. Phys. Solid State **13**, 3023 (1972) [Sov. Phys. JETP **33**, 1053 (1971)].
[45] D. van Tuan, F. Ortmann, D. Soriano, S. O. Valenzuela, and S. Roche, Nat. Phys. **10**, 857 (2014).
[46] T. Yan, X. Qiao, P. Tan, and X. Zhang, arXiv:1502.07088.
[47] Y. Song and H. Dery, Phys. Rev. Lett. **111**, 026601 (2013).
[48] G. Wang, C. Robert, A. Suslu, B. Chen, S. Yang, S. Alamdari, I. C. Gerber, T. Amand, X. Marie, S. Tongay, and B. Urbaszek, arXiv:1506.08114.

[49] A. Arora, M. Koperski, K. Nogajewski, J. Marcus, C. Faugeras, and M. Potemski, arXiv:1503.01682.
[50] B. Ganchev, N. Drummond, I. Aleiner, and V. Fal'ko, Phys. Rev. Lett. **114**, 107401 (2015).
[51] A. Kormányos, V. Zólyomi, N. D. Drummond, and G. Burkard, Phys. Rev. X **4**, 011034 (2014).
[52] N. Kumar, Q. Cui, F. Ceballos, D. He, Y. Wang, and H. Zhao, Phys. Rev. B **89**, 125427 (2014).
[53] Y. You, X.-X. Zhang, T. C. Berkelbach, M. S. Hybertsen, D. R. Reichman, and T. F. Heinz, Nat. Phys. **11**, 477 (2015).
[54] F. Pezzoli, L. Qing, A. Giorgioni, G. Isella, E. Grilli, M. Guzzi, and H. Dery, Phys. Rev. B **88**, 045204 (2013).
[55] C. H. Henry and D. V. Lang, Phys. Rev. B **15**, 989 (1977).
[56] P. C. Sercel, Phys. Rev. B **51**, 14532 (1995).
[57] D. F. Schroeter, D. J. Griffiths, and P. C. Sercel, Phys. Rev. B **54**, 1486 (1996).
[58] R. Fivaz and E. Mooser, Phys. Rev. **163**, 743 (1967).
[59] K. Kaasbjerg, K. S. Bhargavi, and S. S. Kubakaddi, Phys. Rev. B **90**, 165436 (2014).
[60] S.-Y. Chen, C. Zheng, M. S. Fuhrer, and J. Yan, Nano Lett. **15**, 2526 (2015).